

Harnessing Artificial Intelligence for Lung and Colon Cancer Classification via CNN

Zulqarnain Iqbal¹, Adnan Ahmed Rafique^{1*}, Areeba Sarwar¹, and Maryam Izat¹

¹Department of Computer Sciences & Information Technology, University of Poonch Rawalakot, 12350, Pakistan.

*Corresponding Author: Adnan Ahmed Rafique, Email: adnanrafique@upr.edu.pk

Received: June 11, 2024 Accepted: September 29, 2024

Abstract: The aggressiveness, strong propensity to spread, and heterogeneity of cancer seem to be the main causes of its very high fatality rate. Throughout the world, lung and colon cancers are two of the most common malignancies that affect individuals of all ages. Accurate and timely detection of these cancers may improve the best aspects of treatment and increase the survival rate. As a complement to the current cancer detection techniques, an extremely exact and computationally effective model is proposed for the rapid and accurate diagnosis of cancers in the lung and colon area. By employing a cyclic learning rate, the accuracy of the proposed techniques is increased while maintaining their processing efficiency. This is easy to use and effective, which speeds up the model's convergence. Furthermore, many transfer learning models that have already been trained are used and compared with the proposed CNN that has attention layers. The validation, testing, and training of the study make use of the LC25000 dataset. It is observed that the proposed model reduces the impact of inter-class disparities between lung adenocarcinoma and lung cancer of squamous cells by offering higher accuracy. By putting the proposed framework into practice, accuracy was improved to 99.04%.

Keywords: Attention Layers; Convolutional Neural Network; Lung Cancer Pathology; Machine Learning; Transfer Learning.

1. Introduction

All diseases that affect various parts of the body collectively are referred to as malignancies. One feature that distinguishes cancer from other diseases is the unchecked, fast proliferation of aberrant cells that have crossed normal borders and have the potential to infiltrate other organs. The International Agency of Research on Cancer (IARC), which is part of the World Health Organization (also known as the WHO) [1] predicts that, with 19 million additional cases and over 10 million deaths, cancer will be the world's largest cause of death in 2020. The primary cause of cancer-related mortality is metastasis, or the movement of cancer from its original location to a different organ in the human body without the aid of adhesion molecules. All organs in the human body are susceptible to cancer, however, the women's breasts, the colon, the liver, and the stomach are the organs most frequently affected. Among the most common cancers that claim the lives of individuals, lung, and colon cancers are equally common in men and women. Globally, there were 2.21 million new cases of lung cancer, 1.93 million instances of cancer of the colorectal, 1.80 million lung cancer-related deaths, and nearly 1 million colorectal cancer-related deaths in 2020 [2]. Some of the activities that lead to the development of cancer include smoking, having a drinking problem, and having an elevated body mass index. In addition to inherited poisons, physical poisons involve irradiation and UV rays [2]. Mutant lung cells develop uncontrolled until they amalgamate into a mass called a tumor, at which point they become malignant. If there are malignant cells in the colon, which is the final segment of the digestive tract, colon cancer may occur. Most colon cancer cases begin with an uncontrollably growing tumor caused by normal cells lining the colon or rectum. Colon cancer can develop if there are cancerous cells in the colon, which is the last part of our digestive system. The majority of

occurrences of colon cancer start with an uncontrollably expanding tumor that is brought on by healthy cells covering the colon or rectum.

Without a variety of diagnostic techniques, the task of identifying cancer is difficult. Most of the time, patients have little to no signs at all, but when they do, it's frequently too late. Research on metastases is crucial as 90% of cancer deaths are caused by the disease's metastatic spread [3]. While colon cancer typically spreads to the liver, the lungs, and the peritoneum, lung cancer typically expands to the brain, the liver, and other areas of the lungs. Even while symptoms are often linked to the existence of cancerous cells in an organ where they spread, metastatic cells would seem under a microscope to be sick main organ cells [4]. These days, early detection and appropriate treatment are the main tactics for reducing the rate of cancer-related death [5]. For instance, with the appropriate treatment, over 92% of patients with colon cancer between the ages of 18 and 73 who are in Stage 0 may survive; the same is true of 83% of patients who are in Stage 1, 67 percent of people in Phase 2, and 11 percent of people in Stage 3. The equivalent rates of survival for cancer of the lungs are 69 percent, 29 percent, 50 percent, and 8%, according to [6]. The expensive expense of screening technology prevents many individuals from using it. Other than wealthier countries, 70% of cancer-related deaths occur in these other countries [2]. It is feasible that the solution to this issue lies in a field unrelated to medicine. The medical field uses deep learning for a number of purposes [7].

For forty years, the primary goal of the image analysis technique was to categorize histopathological images into patterns that were benign or non-cancerous for investigation, which allowed researchers to study the automatic assisted diagnosis of cancer. However, handling the intricacy of histology images was challenging due to the difficulty of image processing. The concept of autonomous image processing was explored around 40 years ago [8], but the challenge of understanding complicated images remains today. Back then, feature extraction played a crucial role in the development of computer-aided diagnostic (CAD) systems based on machine learning. Numerous tumor models have been examined in research by [9], which by testing different deep learning techniques, offers a comprehensive overview of cancer detection. It also provides comparisons between the several well-known designs. The researcher's earlier works are briefly discussed in the following lines.

In [10], a represented Sparse in the Environment Classification (mSRC) method for lung cancer diagnosis was presented. The authors automatically segmented sections of neurons numbered 4372 of the lung cancer diagnosis using materials from needle biopsies. ... This method's average classification accuracy is 88.10%. The researchers of [11] classified cancer according to the examination of CT scan images using a technique that addressed CAD. They used six different statistical characteristics and two types of networks: forward and reverse propagation. The comprehensive analysis reveals that coupling a skew and ANN to back-propagation yields the best classification results. In [12], a label-free colon cancer classification method was described. This study used several colon cancer dedifferentiation phases and infrared spectrum histopathology imaging. A supervised learning technique called Random Forest (RF), which is based on Decision Trees (DT), was used to categorize the data. A system that can automatically identify polyp from colonic film and evaluate the video to assess malignancy was developed by Yuan et al. and presented in [13]. For categorization, they employed the popular CNN-based design AlexNet, which produced an accuracy rate of 91.47%. A technique for detecting cancer of the lungs stages has been proposed by Masood et al. in [14]. In their investigation, the researchers used CNN and DFCNet, and they evaluated their method on six different datasets. A swarm optimization-based technique for lung cancer diagnosis using images from several sources was presented in [15]. Their favorite learning method, a network of recurrent neural networks (RNN), produced a maximum accuracy rating of 98%.

A neural network-based approach was employed in [16] to categorize binary weights and identify cancer of the colorectal from colonoscopy footage. After evaluation, the collected data had a categorization accuracy of above 90%. An automated method for identifying lung cancer was created in [17]. For the normalization procedure, they employed bin smoothing and a Wolf heuristic selection of features approach. The neuronal network-based collaborative learning research's classification was an especially intriguing aspect of its methodology. It had an accuracy rate of above 99%. In order to accomplish the task of classification, a CNN approach with convolutional layers with values all three pooling two times and single grouping normalizing with dropouts was employed in [18] to extract characteristics from histopathological images of lungs and colon cancer. More than 96.33% of it was accurate.

After over three sets of characteristics were extracted from histopathology images for lung and colon cancer, a CNN model was developed. The author utilized a custom CNN equipped with the Self Attention Layer attention module. The Custom CNN class includes layers including convolutional, activation, pooling, and dropout layers and is derived from PyTorch's nn module. The attention mechanism is implemented by the author through the usage of the Self Attention class, which is employed in the Custom CNN model. It is made up of convolutional layers for query, key, and value in addition to a gamma parameter for sizing.

Thus, it may be decided that the classification system for colorectal and lung tumors has been having a significant impact. Additionally, algorithms based on deep learning with different setups are now exceeding the performance of modern approaches. There is a significant potential for innovation and advancement to be made in this area of research. As machine learning techniques have been used to classify and predict many biological signal types. The development of Deep Learning (DL) algorithms has made it possible for machines to handle data that is high dimensional by nature, such as images and videos. To extract features from pathological images, perform end-to-end training, and gradually and reliably categorize the lung and colon cancer pathological images, a CNN model was created from the ground up. To get the optimal configuration, the Hyperparameters were adjusted, and a cyclical learning method was employed to minimize computation and speed up the model.

The major contributions of our proposed system are as follows:

1. The CNN network model combined with attention layers to enhance performance in lung and colon cancer classification.
2. The cyclical learning rate is incorporated for the improvement of accuracy and a reduction in computational costs.
3. Multiple transfer learning techniques are utilized to improve the accuracy and to compare it with other state-of-the-art techniques.

2. Materials and Methods

2.1. Cyclic Learning Rate

One of the best architectural solutions for the problem of image categorization is the CNN. CNNs use filtering techniques that remove the most distinctive aspects from an image's pixel composition. The most important hyper-parameter to modify when using supervised artificial neural networks is their well-known learning rate. This technique allows the learning rate to cycle among acceptable boundary values instead of dropping monotonically. Training utilizing cyclical learning rates, as opposed to values, often needs fewer rounds and boosts accuracy without requiring the use of a trial-and-error approach. The underlying premise of the cyclical technique is predicated on the notion that learning at a faster pace may have both short- and long-term negative consequences. This result lends credence to the notion that, rather than using a sequentially constant or exponentially decreasing number, the learning rate should be allowed to vary among a range of values. Triangle windows, as seen in Figure 1, were used however they are the easiest functions to understand and contain a combination of linear raising and linear declining.

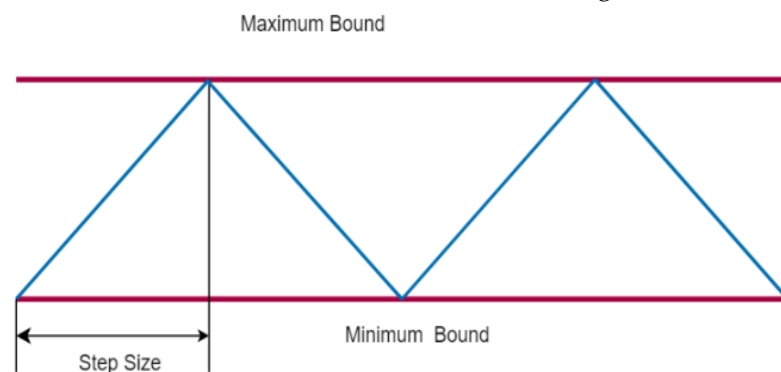


Figure 1. Triangular Learning Rates Policy

In accordance with the learning rate shown in Figure 1, the initial learning rate value was modified to 0.003 as the loss of information decreased after the loss was measured against the learning rate.

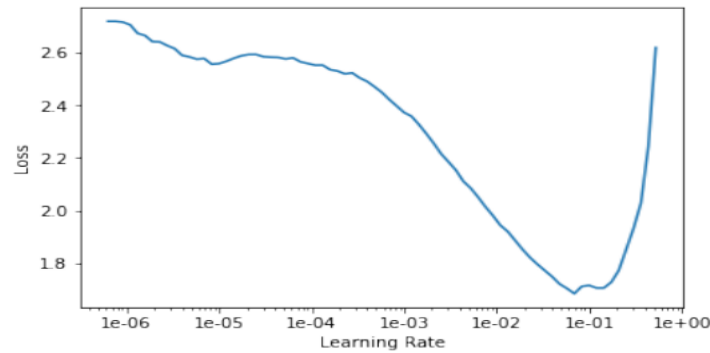


Figure 2. Learning Rate vs Loss (the baseline learning rate)

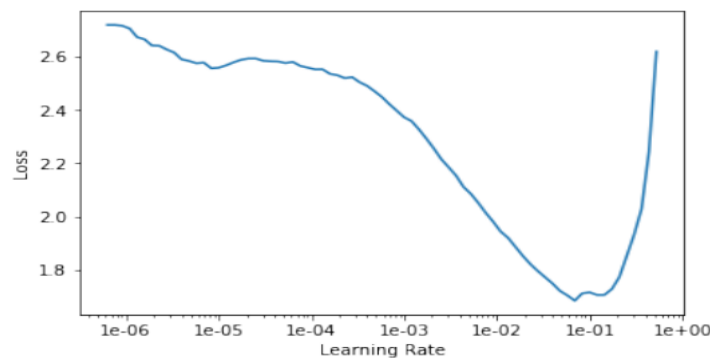


Figure 3. Learning Rate vs Loss

The ideal learning rate is obtained by repeating the cyclical rate for learning following eight training epochs. The difference in rates of learning at the start of reducing loss and at the point where the loss's declination becomes irregular or begins to climb are the ideal restrictions for identifying the base and optimal learning rates, respectively [20]. As a result, figure 3 represents the maximum learning rate, whereas the figure 2 represents the base learning ratio. Using the maximum rate of acquisition fixed at 0.0301 and the starting training parameter set at 0.0045.

2.2. Proposed CNN Architecture

CNNs' ability to recognize local patterns and spatial hierarchies makes them ideal for processing visual input. Convolutional layers make up its structure, which uses filters to extract visual information from input images. Through a series of pooling and convolution layers, these features are gradually acquired, enabling the neural network to collect both high-level and low-level representations. A convolution layer tries to learn filters in a three-dimensional space consisting of one channel dimension and two dimensions of space (width and height). Using this layer required the usage of 64x64 pixel RGB images. As a result, one convolution kernel may be used to map both spatial and cross-channel correlations. Using typical 3x3 and 5x5 convolutions, across-channel connections are placed in these less 3D spaces after the source data is split into up to four smaller regions than the initial input space. This depth-wise convolution is the foundation of the depth-wise separate convolution, often known as a "separable convolution" in deep learning systems. A spatial convolution that is executed independently for every input channel after a pointwise convolution. This is not to be confused with a spatially separate convolution, despite what the term "separable convolution" would imply. Depth-wise separable convolutions are usually executed without nonlinearities, however, a ReLU non-linear nature follows both processes.

Every layer in a network may learn more by itself by using the self-attention layer. Using learned transformations, the attention method usually entails computing the query, key, and value matrices for each element or portion of the input. Determine the attention scores by a compatibility measure between the key vectors and the query. Techniques like concatenated followed by a feed-forward network, scaled dot product, and dot product can be used to accomplish this. To derive attention weights, the attention ratings were normalized using a softmax function. Using the attention weights, calculate the context vector by summing the value vectors in a weighted manner. The attention module is applied after the input has undergone convolution, activation, & pooling processes during the forward pass. After being flattened,

feature maps are routed through layers that are fully linked. The input is passed across the linear layer to get the final output. To execute attention, a Self-attention class computes the energy between the query and the key. The Softmax is then used to produce attention weights, which are then multiplied by the value. After being scaled, the generated feature maps are appended to the input. A regularization method called dropouts keeps the model from overfitting. As dropouts are added, a certain percentage of the network's neurons are randomly altered. The connections between an interneuron and its outgoing neurons are severed when the neuron is switched off. Conventional NNs are designed to replace their completely linked layers with a pooling technique known as max pooling. It is necessary to create a single feature map for every related categorization task category. Following model development, lungs, and colon histopathology images were classified using the softmax activation function.

Convolutional, attention, flatten, and all connected layers are the layers that comprise a CNN's architecture, as seen in Figure 4. Table 2 lists the attributes of our proposed model.

Table 1. Feature Attributes of Proposed Model

Specifications	Values
Input Images	64 x 64 x 3
Convocation_2D Layers Are Activated	ReLu
2D layer of Pooling	3 x 3
Output Layer activation	Soft-Max
compositional optimizer	Adam

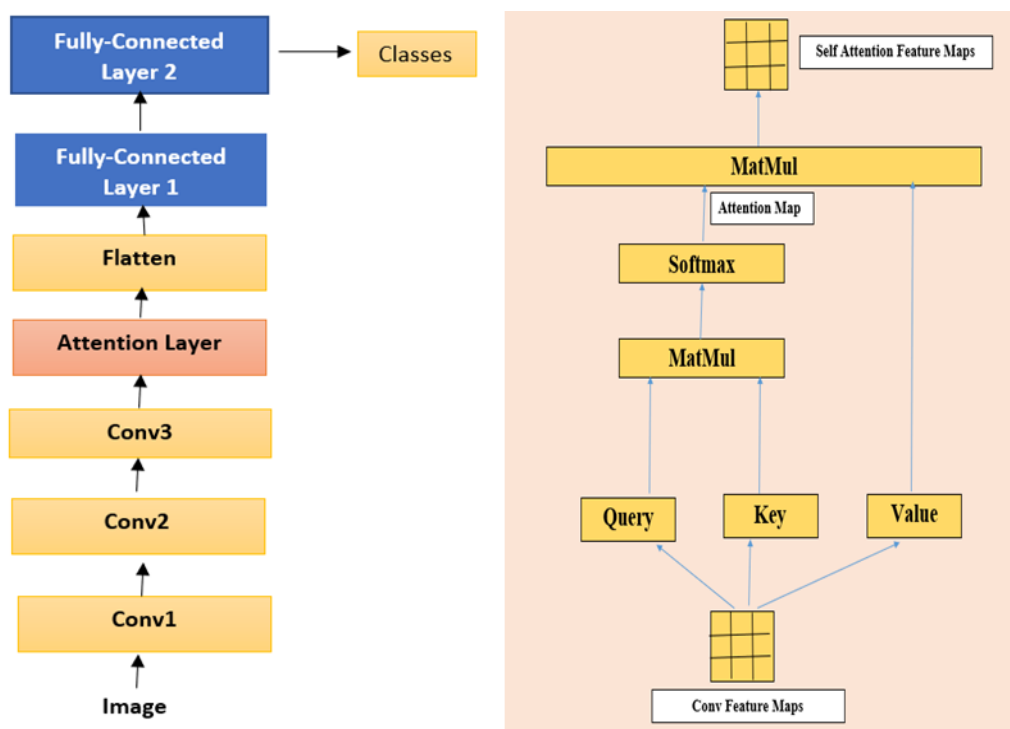


Figure 4. Proposed schematic view of a convolutional neural network

3. Results

3.1. Dataset Description (LC25000)

This dataset contains 25 thousand images that fall into five separate groups [19]. Among these variations are lung cancers such as squamous cell malignancy, harmless tissue from the lungs, normal colonic tissue, lung cancer, or normal tissue from the lung. In all, 1250 images of different malignant tissues

were gathered by the authors (250 images for each category). Several tactics were used to increase the number of images within every class to 5 thousand images in total.

Cutting was done to reduce the initial 1024 or 768 pixels into a single 768 or 768 squares before using augment methods. There are no fees involved in utilizing any of the images in the dataset, which has been verified and complied with. The dataset's contents and class names are listed in Table 1.

Table 2. Description of the LC25000 Dataset

Type of Cancer	Number of Samples
Adenocarcinoma colon	5000
Benign Colon Tissue	5000
Adenocarcinoma Lung	5000
Benign Lung Tissue	5000
Squamous Cell Cancer of the Lungs	5000
Total	25000

A sampling of these five distinct kinds of lungs and colon tissues' histopathological scans, taken from the LC25000 dataset, is displayed in Figure 1.

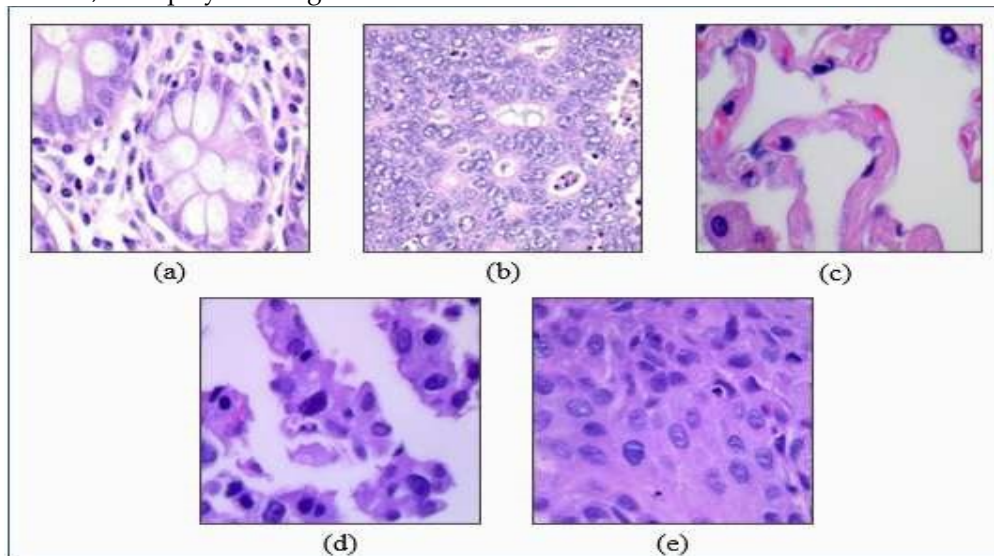


Figure 5. A few examples from the LC25000 dataset

Figure 5 illustrates some example images of the LC25000 dataset containing the following: (a) benign tissue of the colon; (b) adenocarcinoma of the colon; (c) benign tissue of the lung; (d) adenocarcinoma of the lung; and (e) squamous cell carcinoma of the lung.

3.2. Experimental Results and Discussion

This section explains the system variables. The top model's recall, precision, and F1 score stand out among the accuracy metrics. To decide which method is the best to investigate further, the accuracy visuals, confusion matrix, and classifications are evaluated.

Multiclass classification analyses are carried out using LC25000. The down-sampling technique resulted in the image being reduced in size to 64x64. On the LC25000 dataset, some pre-trained transfer learning strategies were also used. The following are the accuracy comparisons between our model and many other transfer learning models.

Figure 6 indicates clearly that the testing accuracy of the proposed model performs better than transfer learning approaches, including those employed by other researchers. In this instance, low-level features retrieved by transfer learning approaches that utilize comparison datasets are not very helpful since histopathology plates and benchmark data sets have relatively different properties.

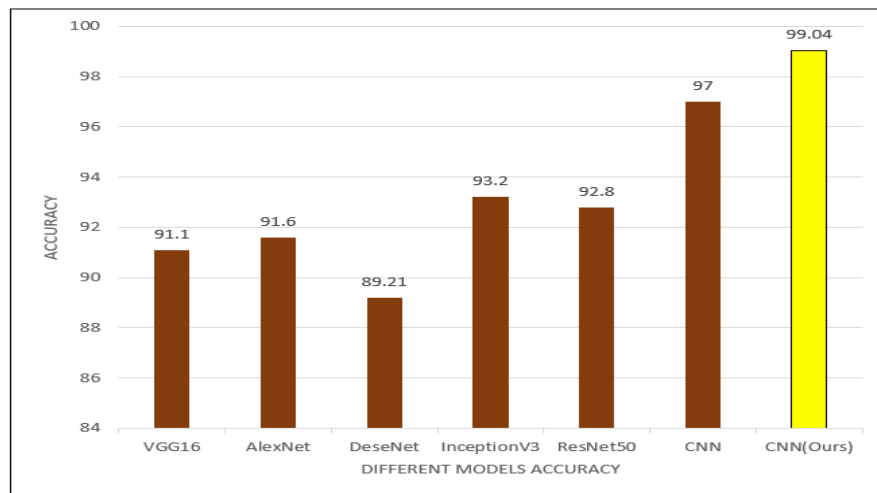


Figure 6. Comparative analysis of the accuracy of various models

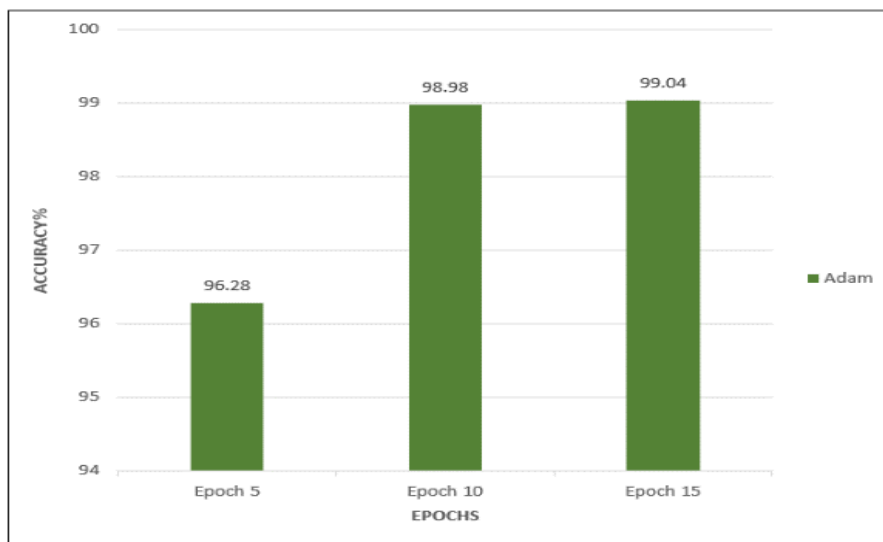


Figure 7. Adam Optimizer Comparison

An optimizing algorithm is an optimization method or function that modifies a neural network's characteristics. It helps reduce overall loss and increase precision. The optimizers mentioned below were applied to this model: Adam, the optimizer

Figure 7 shows that Adam's model forecast accuracy was the greatest; hence, Adam was chosen since, as Figure 6 shows, the model's accuracy was the highest. Figure 8 shows the batch size that was employed, which was determined by the number of samples obtained before the hyper-parameter tuning of the model was processed.

The comparison curve indicated that batch size 32 had the best accuracy among the options, thus that's why it was selected. Table 3 specifics the hyper-parameter configuration for the proposed model.

When the data set is divided, the proposed model keeps the 80:10:10 ratio for training, validation, and testing. The performance of the proposed technique is demonstrated by presenting different parameters in Figures 9 and 10, and the precision of the training and validation phases is displayed in Figure 11.

The experimental results for multiple class classification accuracy are shown in Table 4, where they were evaluated and compared to those of other researchers. The studies were compared using the proposed technique even though they did not all utilize the same dataset, however, the objective of the task was the same. With adenocarcinoma of the lungs and squamous cell carcinoma, the overall classification accuracy was 99.04%, and the inter-class variance was greatly reduced. Table 4 demonstrates the accuracy of the proposed framework is higher as compared to the other models.

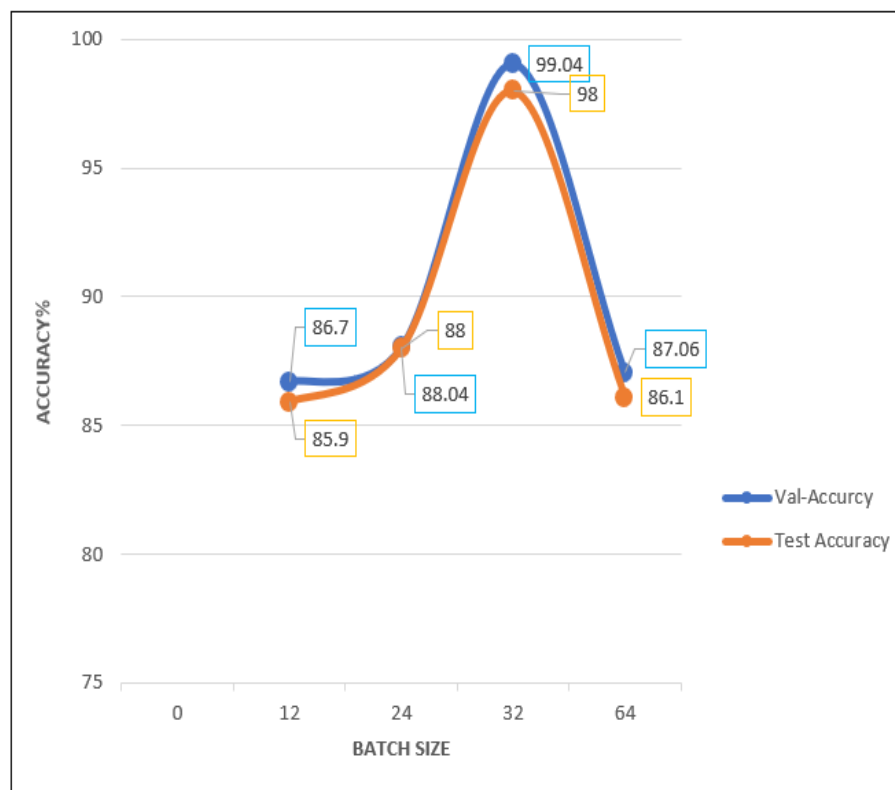


Figure 8. The graph of batch size vs accuracy

Table 3. The hyper-parameter configuration for the proposed model

Parameter	Ranges	Normal Value
Epoch	5,10,15,20,25,30,35,40	20
Batch Size	4,8,16,32,64	32
Optimizer;s	Adam, SGD, RMS-Prop	Adam
Drop-out rate	0.20,0.3, 0.5,.0.40, 0.50	0.5

Accuracy: 99.04%

	precision	recall	f1-score	support
colon_aca	1.00	1.00	1.00	517
colon_n	1.00	1.00	1.00	505
lung_aca	0.98	0.97	0.98	480
lung_n	1.00	1.00	1.00	502
lung_scc	0.98	0.98	0.98	496
accuracy			0.99	2500
macro avg	0.99	0.99	0.99	2500
weighted avg	0.99	0.99	0.99	2500

Figure 9. Report on Dataset Classification for LC2500

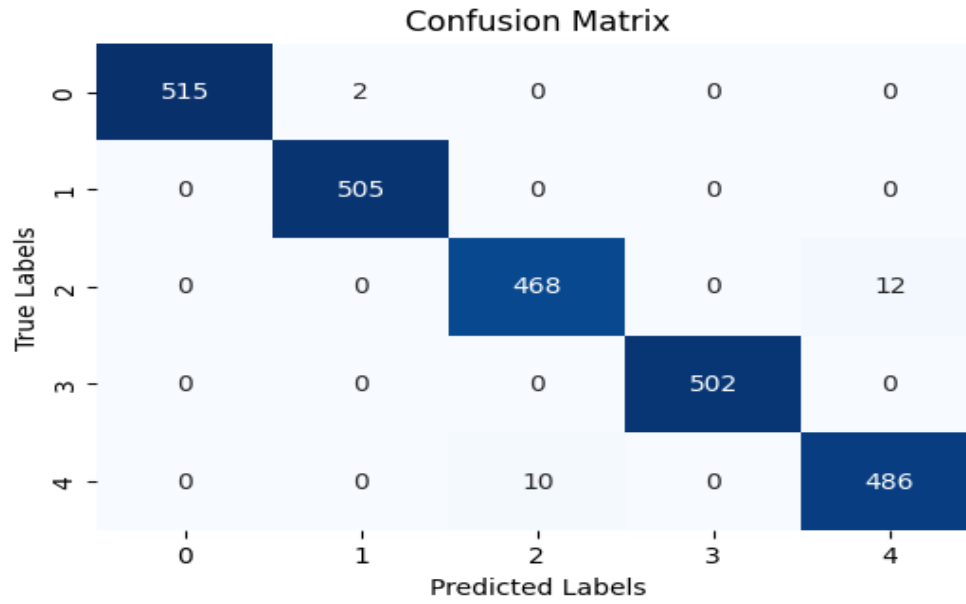


Figure 10. Confusion Matrix for the LC25000 Dataset

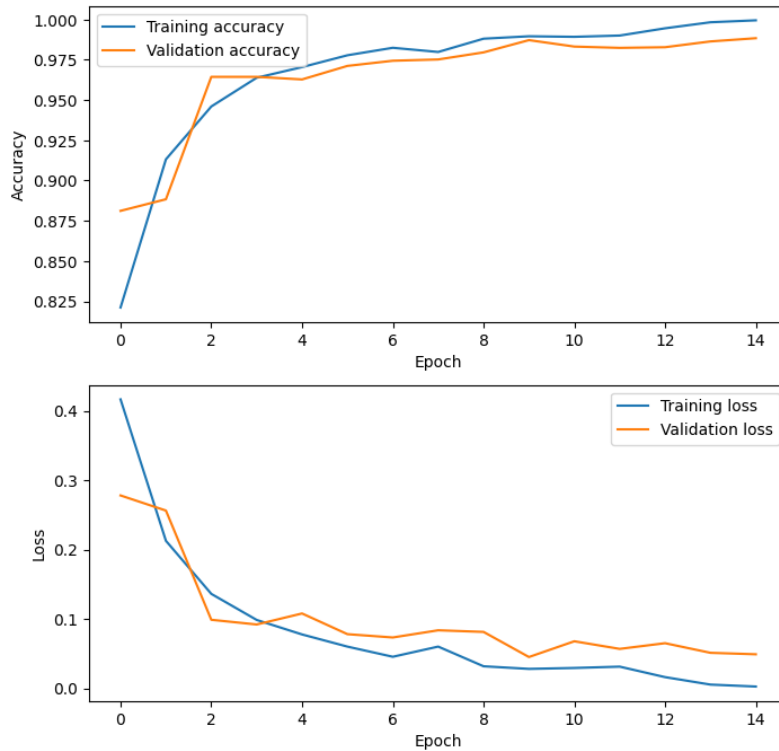


Figure 11. Accuracy Loss Curves for Training and Validation

Table 4. The performance comparison of the proposed model with other state-of-the-art methods.

Author	Type of Images	Model	Accuracy	Precision	Recall	F1 Score
Shi. Y et al. [21],	Biopsy Images	m-SRC	88.2	0.845	0.912	0.877
Xu. y et al. [22],	Histopathological	SVM's	--	0.738	0.683	0.709
Kuruvilla. Y et al. [23],	CT Scan	ANN	93.2	--	0.913	--
Sirinukunwattana Y et al. [24],	Histopathological	CNN	--	0.783	0.827	0.804
Kuepper. Y et al. [25],	Histopathological	RF	95.2	--	0.942	--
W. She. et.al. [26],	CT Scan	CNN	87.12	--	0.930	--
Z.Yun et.al. [13],	Colonoscopy	Alex-Net	87.15	--	0.918	--
T.Bab et al. [27],	Histopathological	RF	85.4	--	--	--

M. Akbar et al. [28],	Colonoscopy	CNN	90.23	0.743	0.683	0.712
Sursh. et al. [29],	CT Scan	CNN	93.9	--	0.935	--
M.Masud et al. [30]	Histopathological	CNN	96.37	0.963	0.963	0.963
M.A Provath et al. [31]	Histopathological	CNN	97	0.970	0.970	0.970
Proposed	Histopathological	CNN	99.04	0.990	0.990	0.990

4. Conclusions

Lung and colon cancers are thought to be the most prevalent types of cancer among all others. Early cancer identification can increase a patient's chances of survival. The primary objective of the proposed strategy was to provide these two cancer kinds with a more robust and reliable methodology. This finding was achieved by applying CNN-based models to a collection of 25,000 histological images of lungs and colon tissues. Accuracy increased to 99% when the Custom CNN and attention layers technique were used together. Compared to existing techniques, the proposed methodology for identifying lung and colon cancer gives more accuracy. Every trial demonstrates how successful the proposed approach is in identifying cancer. We presented a highly automated deep learning-based approach to the diagnosis of lung and colon cancer. We demonstrated how CNN from the classification region of the image when paired with attention layers, might be a useful tool for classifying colon and lung cancer. Our model had the best accuracy, at 99.04%. Utilizing the relationships between various parts of the original X-ray image, we applied the CNN + Attention layer approach for the illness categorization.. Experiment results show that the proposed strategy performs better in lung and colon cancer classification than previous state-of-the-art methods. We intend to segment images using the scratch CNN algorithm in the future in order to increase classification accuracy and investigate more image attributes.

Funding: This research received no external funding

Conflicts of Interest: The authors declare no conflict of interest.

References

1. I. A. for Research on Cancer, "World Fact Sheet," <https://gco.iarc.fr/today/data/factsheets/populations/900-world-fact-sheets.pdf/>, 2020, accessed 26-June-2022.
2. I. H. Organization, "Cancer," <https://www.who.int/news-room/fact-sheets/detail/cancer/>, 2022, accessed 26-June-2022.
3. Sajjad, R., Khan, M. F., Nawaz, A., Ali, M. T., & Adil, M. (2022). Systematic Analysis of Ovarian Cancer Empowered with Machine and Deep Learning: A Taxonomy and Future Challenges. *Journal of Computing & Biomedical Informatics*, 3(02), 64-87.
4. T. N. Seyfried and L. C. Huysentruyt, "On the origin of cancer metastasis," *Critical Reviews™ in Oncogenesis*, vol. 18, no. 1-2, 2013.
5. Verywellhealth, "What Is Metastasis?" <https://www.verywellhealth.com/metastatic-cancer-2249128/>, 2022, accessed 27-June-2022.
6. L. F. S´anchez-Peralta, L. Bote-Curiel, A. Pic´on, F. M. S´anchez-Margallo, and J. B. Pagador, "Deep learning to find colorectal polyps in colonoscopy: A systematic literature review," *Artificial Intelligence in Medicine*, vol. 108, p. 101923, 2020.
7. C. Health, "Cancer Survival Rates," <https://cancersurvivalrates.com/?type=colon&role=patient/>, 2022, accessed 26-June-2022.
8. S. Das, S. Biswas, A. Paul, and A. Dey, "Ai doctor: An intelligent approach for medical diagnosis," in *Industry Interactive Innovations in Science, Engineering and Technology*, S. Bhattacharyya, S. Sen, M. Dutta, P. Biswas, and H. Chattopadhyay, Eds. Singapore: Springer Singapore, 2018, pp. 173–183.
9. K. Doi, "Computer-aided diagnosis in medical imaging: Historical review, current status and future potential," *Computerized Medical Imaging and Graphics*, vol. 31, no. 4, pp. 198–211, 2007, computer-aided Diagnosis (CAD) and Image-guided Decision Support.
10. Ejaz, F., Ahmad, A., & Hanif, K. (2020). Prevalence of diabetic foot ulcer in lahore, Pakistan: a cross sectional study. *Asian Journal of Allied Health Sciences (AJAHS)*, 34-38.
11. G. M. te Brake, N. Karssemeijer, and J. H. Hendriks, "An automatic method to discriminate malignant masses from normal tissue in digital mammograms1," *Physics in Medicine & Biology*, vol. 45, no. p. 2843, 2000.
12. Y. Shi, Y. Gao, Y. Yang, Y. Zhang, and D. Wang, "Multimodal sparse representation-based classification for lung needle biopsy images," *IEEE Transactions on Biomedical Engineering*, vol. 60, no. 10, pp. 2675–2685, 2013.
13. J. Kuruvilla and K. Gunavathi, "Lung cancer classification using neural networks for ct images," *Computer methods and programs in biomedicine*, vol. 113, no. 1, pp. 202–209, 2014.
14. C. Kuepper, F. Großerueschkamp, A. Kallenbach-Thieltges, A. Mosig, A. Tannapfel, and K. Gerwert, "Label-free classification of colon cancer grading using infrared spectral histopathology," *Faraday Discussions*, vol. 187, pp. 105–118, Jan. 2016.
15. Z. Yuan, M. Izady Yazdanabadi, D. Mokkaapati, R. Panvalkar, J. Y. Shin, N. Tajbakhsh, S. Gurudu, and J. Liang, "Automatic polyp detection in colonoscopy videos," in *Medical Imaging 2017: Image Processing*, vol. 10133. SPIE, 2017, pp. 718–727.
16. A. Masood, B. Sheng, P. Li, X. Hou, X. Wei, J. Qin, and D. Feng, "Computer-assisted decision support system in pulmonary cancer detection and stage classification on ct images," *Journal of Biomedical Informatics*, vol. 79, pp. 117–128, 2018.
17. R. Selvanambi, J. Natarajan, M. Karuppiah, S. H. Islam, M. M. Hassan, and G. Fortino, "Lung cancer prediction using higher-order recurrent neural network based on glowworm swarm optimization," *Neural Computing and Applications*, vol. 32, pp. 4373–4386, 2020.
18. M. Akbari, M. Mohrekesh, S. Rafiei, S. R. Soroushmehr, N. Karimi, S. Samavi, and K. Najarian, "Classification of informative frames in colonoscopy videos using convolutional neural networks with binarized weights," in *2018 40th annual international conference of the IEEE engineering in medicine and biology society (EMBC)*. IEEE, 2018, pp. 65–68.
19. P. M. Shakeel, A. Tolba, Z. Al-Makhadmeh, and M. M. Jaber, "Automatic detection of lung cancer from biomedical data set using discrete adaboost optimized ensemble learning generalized neural networks," *Neural Computing and Applications*, vol. 32, pp. 777–790, 2020.
18. M. Masud, N. Sikder, A.-A. Nahid, A. K. Bairagi, and M. A. AlZain, "A machine learning approach to diagnosing lung and colon cancer using a deep learning-based classification framework," *Sensors*, vol. 21, no. 3, p. 748, 2021.

20. A. A. Borkowski, M. M. Bui, L. B. Thomas, C. P. Wilson, L. A. DeLand, and S. M. Mastorides, "Lung and colon cancer histopathological image dataset (lc25000)," arXiv preprint arXiv:1912.12142, 2019.
21. L. N. Smith, "Cyclical learning rates for training neural networks," in 2017 IEEE Winter Conference on Applications of Computer Vision (WACV), 2017, pp. 464–472.
22. Y. Shi, Y. Gao, Y. Yang, Y. Zhang, and D. Wang, "Multimodal sparse representation-based classification for lung needle biopsy images," IEEE Transactions on Biomedical Engineering, vol. 60, no. 10, pp. 2675–2685, 2013.
23. Y. Xu, L. Jiao, S. Wang, J. Wei, Y. Fan, M. Lai, and E. I.-c. Chang, "Multi-label classification for colon cancer using histopathological images," Microscopy Research and Technique, vol. 76, no. 12, pp. 1266–1277, 2013.
24. J. Kuruvilla and K. Gunavathi, "Lung cancer classification using neural networks for ct images," Computer methods and programs in biomedicine, vol. 113, no. 1, pp. 202–209, 2014.
25. K. Sirinukunwattana, S. E. A. Raza, Y.-W. Tsang, D. R. Snead, I. A. Cree, and N. M. Rajpoot, "Locality sensitive deep learning for detection and classification of nuclei in routine colon cancer histology images," IEEE transactions on medical imaging, vol. 35, no. 5, pp. 1196–1206, 2016.
26. C. Kuepper, F. Großerueschkamp, A. Kallenbach-Thieltges, A. Mosig, A. Tannapfel, and K. Gerwert, "Label-free classification of colon cancer grading using infrared spectral histopathology," Faraday discussions, vol. 187, pp. 105–118, 2016.
27. W. Shen, M. Zhou, F. Yang, D. Yu, D. Dong, C. Yang, Y. Zang, and J. Tian, "Multi-crop convolutional neural networks for lung nodule malignancy suspiciousness classification," Pattern Recognition, vol. 61, pp. 663–673, 2017.
28. T. Babu, D. Gupta, T. Singh, and S. Hameed, "Colon cancer prediction on different magnified colon biopsy images," in 2018 Tenth International Conference on Advanced Computing (ICoAC). IEEE, 2018, pp. 277–280.
29. M. Akbari, M. Mohrekesh, S. Rafiei, S. R. Soroushmehr, N. Karimi, S. Samavi, and K. Najarian, "Classification of informative frames in colonoscopy videos using convolutional neural networks with binarized weights," in 2018 40th annual international conference of the IEEE engineering in medicine and biology society (EMBC). IEEE, 2018, pp. 65–68.
30. S. Suresh and S. Mohan, "Roi-based feature learning for efficient true positive prediction using convolutional neural network for lung cancer diagnosis," Neural Computing and Applications, vol. 32, no. 20, pp. 15 989–16 009, 2020.
31. M. Masud, G. Muhammad, M. S. Hossain, H. Alhumyani, S. S. Alshamrani, O. Cheikhrouhou, and S. Ibrahim, "Light deep model for pulmonary nodule detection from ct scan images for mobile devices," Wireless Communications and Mobile Computing, vol. 2020, pp. 1–8, 2020.
32. Al-Mamun Provath, M., Deb, K., Jo, KH. (2023). Classification of Lung and Colon Cancer Using Deep Learning Method. In: Na, I., Irie, G. (eds) Frontiers of Computer Vision. IW-FCV 2023. Communications in Computer and Information Science, vol 1857. Springer.